Approximate Closed-form Solutions for the Maxwell-Bloch Equations via the Optimal Homotopy Asymptotic Method

Remus-Daniel Ene[1,*], Nicolina Pop[2], Marioara Lapadat[1] and Luisa Dungan[3]
[1]Department of Mathematics, Politehnica University of Timisoara, 2 Victoria Square, 300006 Timisoara, Romania
[2]Department of Physical Foundations of Engineering, Politehnica University of Timisoara, 2 Vasile Parvan Blvd, 300223 Timisoara, Romania
e-mails: remus.ene@upt.ro, nicolina.pop@upt.ro, maria.lapadat@upt.ro, luisa.dungan@upt.ro
[3]Mech Machines Equipment & Transports Dept, Politehnica University of Timisoara, 300222 Timisoara, Romania; luisa.dungan@upt.ro
*corresponding author: remus.ene@upt.ro

Abstract

This work emphasizes some geometrical properties of the Maxwell–Bloch equations. Based on these properties the closed-form solutions of their equations are established. Thus, the Maxwell–Bloch equations are reduced to a nonlinear differential equation depending on an auxiliary unknown function. The approximate analytical solutions were built using the Optimal Homotopy Asymptotic Method (OHAM). A good agreement between the analytical and corresponding numerical results was found. The accuracy of the obtained results is validated through the representative figures. This procedure could be successfully applied for more dynamical systems with geometrical properties. [1]

1 Introduction

The study of dynamical systems was explored related their important applications in electrical engineering, medicine or economics, such as: complete synchronization or optimization of nonlinear system performance, secure communications,

[1]Mathematical Subject Classification(2008): *65L60*, *76A10*, *76D05*, *76D10*, *76M55*

Keywords and phrases: *optimal homotopy asymptotic method; Maxwell–Bloch equations; symmetries; Hamilton–Poisson realization; periodical orbits.*

and so on. The stabilization of the T system via linear controls was explored in [1]. The Rikitake two-disk dynamo system was studed by [2] and applied in modeling the reversals of the Earth's magnetic field [[3], [4]]. Other the geometrical properties of the dynamical systems, such as integrable deformations, the equilibria points, Hamiltonian realization was analyzed in [[5]-[21]].

The interaction between laser light and a material sample composed of two-level atoms is described by Maxwell equations of the electric field and Schrodinger equations for the probability amplitudes of the atomic levels. The Maxwell-Bloch equations were obtained by coupling the Maxwell equations with the Bloch equation and their important geometrical properties were explored in [[22]-[32]], and so on.

An important geometrical properties of the dynamical system is the existence of symmetries. As it is well-known a dynamical system admits symmetry with respect to the origin point $O(0,0,0)$ or with the $Oz-$ axis or the plan $z=0$ if it is invariant under the transformation $(x,y,z) \rightarrow (-x,-y,-z)$, respectively $(x,y,z) \rightarrow (-x,-y,z)$ and $(x,y,z) \rightarrow (x,y,-z)$.

2 The Maxwell-Bloch equations

2.1 Hamilton-Poisson realization

The real-valued Maxwell-Bloch equations are (see [[33]-[36]]):

$$\begin{cases} \dot{x} = y \\ \dot{y} = x \cdot z \\ \dot{z} = -x \cdot y \end{cases} , \tag{1}$$

where the unknown functions x, y and z depend on $t > 0$ and $\dot{x}$ denotes derivative of the function x with respect to t.

Remark 1. Is easy to see that the considered system admits a symmetries with respect to $Oz-$ axis.

In this section we also recall [35] some geometrical properties of the system (1).

The considered system has a Hamilton-Poisson realization with the Hamiltonian $H(x,y,z) = \frac{1}{2}(y^2+z^2)$ and a Casimir given $C(x,y,z) = z + \frac{1}{2}x^2$.

Remark 2. If the initial conditions are

$$x(0) = x_0 \quad , \quad y(0) = y_0 \quad , \quad z(0) = z_0 \ , \tag{2}$$

then the phase curves of dynamics (1) are the intersections of the surfaces $\frac{1}{2}(y^2+z^2) = \frac{1}{2}(y_0^2+z_0^2)$ and $z + \frac{1}{2}x^2 = z_0 + \frac{1}{2}x_0^2$.

2.2 Closed-form solutions

In this section we establish the closed-form solutions of the system Eq. (1) using previously result.

Making the transformations:

$$\begin{cases} y = R \cdot \sqrt{2} \cdot \sin(v(t)) \\ z = R \cdot \sqrt{2} \cdot \cos(v(t)) \end{cases} , \quad R = \sqrt{\frac{1}{2} \cdot (y_0^2 + z_0^2)} \ , \tag{3}$$

where $v(t)$ is an unknown smooth function, then the second equation from Eq. (1) yields to

$$x = \dot{v}(t). \tag{4}$$

Now, using the first equation from Eq. (1) we obtain:

$$\ddot{v}(t) - R \cdot \sqrt{2} \cdot \sin(v(t)) = 0 \ . \tag{5}$$

Using the initial conditions Eq. (2) and the relations Eqs. (3)-(4) the initial conditions $v(0)$ and $v'(0)$ become:

$$v(0) = \arctan \frac{y_0}{z_0} \quad , \quad v'(0) = x_0, \quad \text{for} \quad z_0 \neq 0 \ . \tag{6}$$

Remark 3. The relations Eqs. (3) and (4) give closed-form solution of the system Eq. (1).

In the last decades there are several analytical methods for solving the nonlinear differential problem given by Eqs. (5)-(6), such as: the Function Method [37], the Multiple Scales Technique [38], the Optimal Homotopy Perturbation Method (OHPM) [39], [40], the Least Squares Differential Quadrature Method [41], the Polynomial Least Squares Method [42], the Optimal Iteration Parametrization Method (OIPM) [43], the Optimal Homotopy Asymptotic Method (OHAM) [44], the Homotopy Perturbation Method (HPM) and the Homotopy Analysis Method (HAM) [45], the Variational Iteration Method (VIM) [46], the Optimal Variational Iteration Method (OVIM) [47].

The approximate analytic solutions of the nonlinear differential problem given by Eqs. (5)-(6) are analytically solved using the Optimal Homotopy Asymptotic Method (OHAM).

3 Basic ideas of the OHAM technique

The general form for the nonlinear differential equation is chosen as [48]:

$$\mathcal{L}\Big(F(t)\Big) + \mathcal{N}\Big(F(t)\Big) = 0, \tag{7}$$

with the boundary / initial conditions

$$\mathcal{B}\Big(F(t), \frac{dF(t)}{dt}\Big) = 0, \tag{8}$$

where $\mathcal{L}$ is an arbitrary linear operator, $\mathcal{N}$ is the corresponding nonlinear operator and $\mathcal{B}$ is an operator characterizing the boundary conditions.

Taking into account of homotopic relation given by:

$$\begin{aligned}&\mathcal{H}\Big[\mathcal{L}\Big(F(t,p)\Big),\ H(t,C_i),\ \mathcal{N}\Big(F(t,p)\Big)\Big] =\\ &= \mathcal{L}\Big(F_0(t)\Big) + p\Big[\mathcal{L}\Big(F_1(t,C_i)\Big) - H(t,C_i)\mathcal{N}\Big(F_0(t)\Big)\Big] = 0,\end{aligned} \tag{9}$$

where $p \in [0,\ 1]$ is the embedding parameter and $H(t,C_i) \neq 0$ is an auxiliary convergence-control function depending of the variable t and of the parameters C_1, C_2, ..., C_s, with the unknown function $F(t,p)$ in the form:

$$F(t,p) = F_0(t) + pF_1(t,C_i), \tag{10}$$

and equating the coefficients of p^0 and p^1, respectively, the deformations problems are obtained.
These are:
- *the zeroth-order deformation problem*

$$\mathcal{L}\Big(F_0(t)\Big) = 0, \qquad \mathcal{B}\Big(F_0(t), \frac{dF_0(t)}{dt}\Big) = 0, \tag{11}$$

- *the first-order deformation problem*

$$\begin{aligned}&\mathcal{L}\Big(F_1(t,C_i)\Big) = H(t,C_i)\mathcal{N}\Big(F_0(t)\Big),\\ &\mathcal{B}\Big(F_1(t,C_i), \tfrac{dF_1(t,C_i)}{dt}\Big) = 0, \quad i = 1,2,...,s.\end{aligned} \tag{12}$$

By solving the linear Eq. (11) the initial approximation could be obtain.

In order to compute $F_1(t,C_i)$ by Eq. (12), taking into account the fact that the nonlinear operator $\mathcal{N}$ has the general form:

$$\mathcal{N}\left(F_0(t)\right) = \textstyle\sum_{i=1}^{n} h_i(t)g_i(t), \tag{13}$$

where n is a positive integer, and $h_i(t)$ and $g_i(t)$ are known functions that depend on $F_0(t)$ and on $\mathcal{N}$.

Following the procedure described in [48], the computation of the function $F_1(t,C_i)$ has the form:

$$F_1(t,C_i) = \textstyle\sum_{i=1}^{m} H_i(t,h_j(t),C_j)g_i(t), \quad j = 1,\ ...,\ s, \tag{14}$$

 doi:10.20944/preprints202209.0474.v1

or

$$F_1(t, C_i) = \sum_{i=1}^{m} H_i(t, g_j(t), C_j) h_i(t), \quad j = 1, \ ..., \ s,$$
$$\mathcal{B}\left(F_1(t, C_i), \ \frac{dF_1(t, C_i)}{dt}\right) = 0. \tag{15}$$

The above expressions of $H_i(t, h_j(t), C_j)$ contain linear combinations of the functions h_j, $j = 1, \ ..., \ s$ and the parameters C_j, $j = 1, \ ..., \ s$. The summation limit m is an arbitrary positive integer number.

For $p = 1$, the first-order analytical approximate solution of Eqs. (7) - (8), taking into account Eq. (10), is:

$$\overline{F}(t, C_i) = F(t, 1) = F_0(t) + F_1(t, C_i). \tag{16}$$

The convergence-control parameters C_1, C_2, ..., C_s can be optimally identified by means of various methods, such as: the Galerkin method, the least square method, the collocation method, the Kantorowich method, or the weighted residual method.

The first-order approximate solution (16) is well-determined if the convergence-control parameters are known.

4 Approximate analytic solutions via OHAM

For the unknown function v the approximate solutions of Eq. (5) with initial conditions given by Eq. (6) are obtaining.

The linear operator $\mathcal{L}\Big(v\Big)$ has the following expression:

$$\mathcal{L}\Big(v\Big)(t) = v'' + \omega_0^2 v, \tag{17}$$

where $\omega_0 > 0$ is an unknown parameter at this moment. Therefore the form of the nonlinear operator $\mathcal{N}\Big(v\Big)$ corresponding to the unknown function v is obtained from Eq. (5) by:

$$\mathcal{N}\Big(v\Big)(t) = -\omega_0^2 v - R\sqrt{2} \cdot \sin\left(v\right) \ , \tag{18}$$

and using the power series expansion

$$\sin\left(v\right) = \sum_{i=0}^{\infty} \left(-1\right)^i \cdot \frac{v^{2i+1}}{(2i+1)!} \ , \tag{19}$$

There are a lot of possibilities to choose the auxiliary function $H(t, C_i)$, one of them could be:

$$H(t, C_i) = C, \tag{20}$$

or

$$H(t,C_i) = C_1\ \cos(\omega_0 t) + B_1\ \sin(\omega_0 t),$$

or

$$H(t,C_i) = C_1\ \cos(\omega_0 t) + B_1\ \sin(\omega_0 t) + C_2\ \cos(3\omega_0 t) + B_2\ \sin(3\omega_0 t),$$

or

$$H(t,C_i) = C_1\ \cos(\omega_0 t) + B_1\ \sin(\omega_0 t) + C_2\ \cos(3\omega_0 t) + B_2\ \sin(3\omega_0 t) + \\ + C_3\ \cos(5\omega_0 t) + B_3\ \sin(5\omega_0 t),$$

and so on.

The zeroth-order deformation problem

For the initial approximation v_0, the Eq. (11) becomes:

$$v'' + \omega_0^2 v = 0, \quad v(0) = \arctan \frac{y_0}{z_0} \ , \quad v'(0) = x_0 \tag{21}$$

with the solution

$$v_0(t) = v(0)\ \cos(\omega_0 t) + \frac{v'(0)}{\omega_0}\ \sin(\omega_0 t). \tag{22}$$

The first-order deformation problem

For the initial approximation $v_0(t)$ given by Eq. (22), using Eq. (19) the nonlinear operator Eq. (18) becomes:

$$\mathcal{N}(v_0)(t) = -\omega_0^2\Big(v(0)\ \cos(\omega_0 t) + \tfrac{v'(0)}{\omega_0}\ \sin(\omega_0 t)\Big) + \\ + \sum_{i=1}^{\infty} \frac{(-1)^i}{(2i+1)!} \cdot \Big(v(0)\ \cos(\omega_0 t) + \frac{v'(0)}{\omega_0}\ \sin(\omega_0 t)\Big)^{2i+1}, \tag{23}$$

and depend on the elementary functions $\cos((2k+1)\omega_0 t)$, $\sin((2k+1)\omega_0 t)$, $k = 1,\ 2,\ 3,\ \cdots$.

For $H(t,C_i)$ choosing the expression given by Eq. 20, for the first-order deformation problem given by Eq. (12), by integration the first approximation $v_1(t,D_i)$, from Eq. (14), becomes:

$$v_1(t,C_i) = \sum_{k=1}^{\infty} C_k \cdot \cos((2k+1)\omega_0 t) + B_k \cdot \sin((2k+1)\omega_0 t), \tag{24}$$

where $C_i,\ B_i$ are unknown parameters, which $\displaystyle\sum_{k=1}^{\infty} B_k \ = 0.$

The first-order analytical approximate solution $\bar{v}$

From Eqs. (22) and (24) the first-order approximate solution given by Eq. (16) is obtained:

$$\begin{aligned}\bar{v}(t) = v_0(t) + v_1(t, C_i) = v(0)\ \cos(\omega_0 t) + \frac{v'(0)}{\omega_0}\ \sin(\omega_0 t) + \\ + \sum_{k=1}^{\infty} C_k \cdot \cos((2k+1)\omega_0 t) + B_k \cdot \sin((2k+1)\omega_0 t)\ ,\end{aligned} \tag{25}$$

where the unknown parameters $C_i,\ B_i,\ i = 1,\ 2,\ 3,\ \cdots$, are optimally identified.

5 Numerical results and Discussions

In this section, we discuss the accuracy of this method by taking into consideration the first-order approximate solution given by Eq. (25) in following form:

$$\begin{aligned}\bar{v}(t) = v_0(t) + v_1(t, C_i) = v(0)\ \cos(\omega_0 t) + \frac{v'(0)}{\omega 0}\ \sin(\omega_0 t) + \\ + \sum_{k=1}^{N_{max}} C_k \cdot \cos((2k+1)\omega_0 t) + B_k \cdot \sin((2k+1)\omega_0 t)\ ,\end{aligned} \tag{26}$$

where $N_{max} \in \{5,\ 10,\ 20,\ 25\}$ is an arbitrary fixed positive integer number.

By means of the Eqs. (3), (4) and (26), the approximate closed-form solutions of the Maxwell-Bloch equations are well-determined, via OHAM technique.

The accuracy of the obtained results is shown in Figs. 1 - 4 and Tables 1-2 by comparison of the above obtained approximate solutions with the corresponding numerical integration results, computed by means of the shooting method combined with fourth-order Runge-Kutta method using Wolfram Mathematica 9.0 software. The convergence-control parameters $C_i,\ B_i,\ i = 1,\ 2,\ 3,\ \cdots\ N_{max}$, which appear in Eq. (26), are computed by the least square method for different values of the known parameter N_{max}. From these Figures we can notice that there are the symmetry with respect to the $Oz-$ axis. The Fig. 5 highlights the symmetry of the 3D trajectory.

The influence of the index number N_{max} on the values of the relative errors is examined in Table 3. The better approximate analytical solution corresponds to the value $N_{max} = 25$. This value was chosen for the efficiency of the solution.

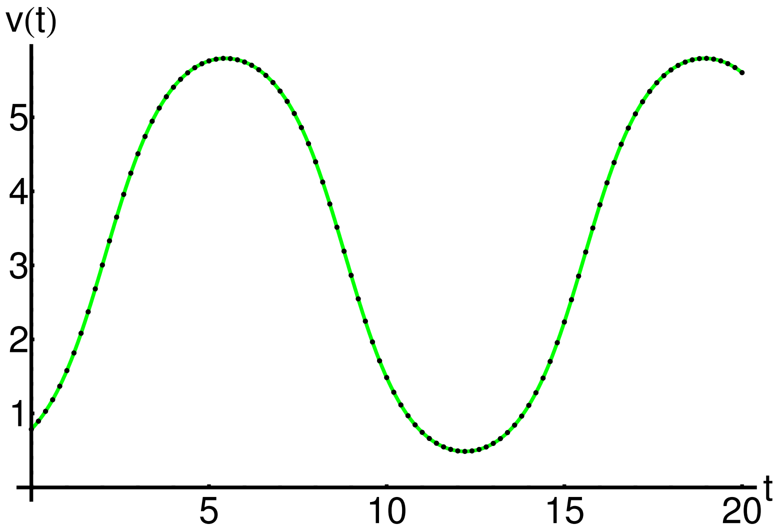

Figure 1: The auxiliary function $\bar{v}(t)$ given by Eq. (26) using the initial conditions $x_0 = 0.5$, $y_0 = 0.5$, $z_0 = 0.5$ for $N_{max} = 25$:
OHAM solution (with lines) and numerical solution (dashing lines), respectively.

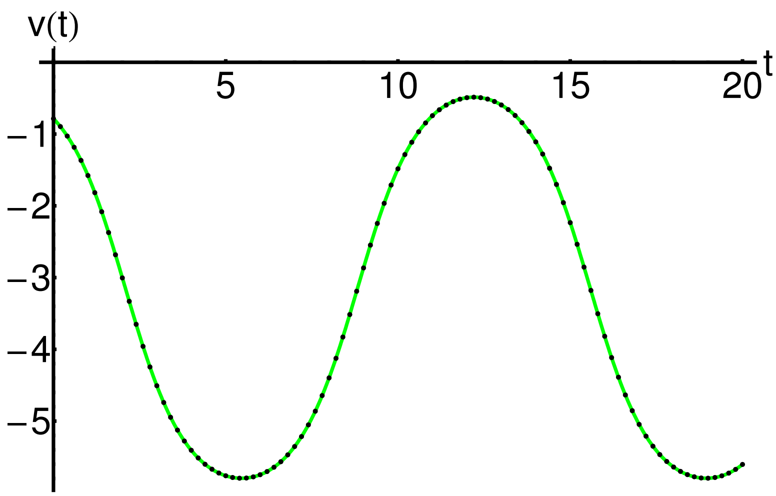

Figure 2: The auxiliary function $\bar{v}(t)$ given by Eq. 26 using the initial conditions $x_0 = -0.5$, $y_0 = -0.5$, $z_0 = 0.5$ for $N_{max} = 25$:
OHAM solution (with lines) and numerical solution (dashing lines), respectively.

6 Conclusions

In the present paper, some geometrical properties of the Maxwell-Bloch equa-

Preprints (www.preprints.org) | NOT PEER-REVIEWED | Posted: 30 September 2022 doi:10.20944/preprints202209.0474.v1

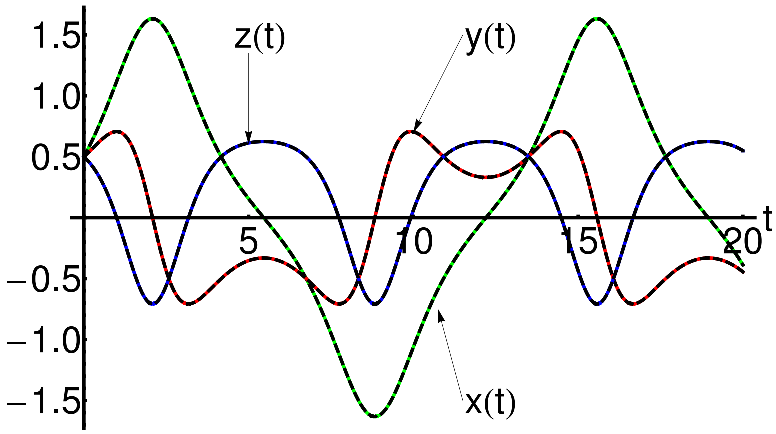

Figure 3: The set of solutions $x(t)$, $y(t)$, $z(t)$ given by Eqs. (3), (4) using Eq. (26) with the initial conditions $x_0 = 0.5$, $y_0 = 0.5$, $z_0 = 0.5$ for $N_{max} = 25$:
OHAM solution (with lines) and numerical solution (dashing lines), respectively.

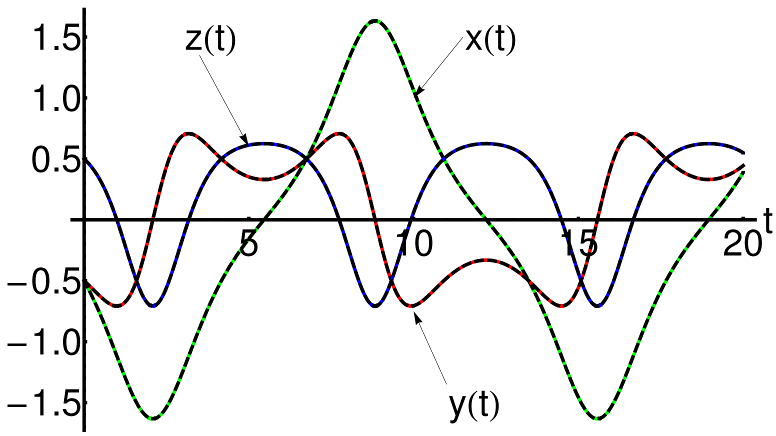

Figure 4: The set of solutions $x(t)$, $y(t)$, $z(t)$ given by Eqs. (3), (4) using Eq. (26) with the initial conditions $x_0 = -0.5$, $y_0 = -0.5$, $z_0 = 0.5$ for $N_{max} = 25$:
OHAM solution (with lines) and numerical solution (dashing lines), respectively.

tions are emphasized and the approximate analytic solutions were established. A good agreement between the approximate analytic solutions (using OHAM) and corresponding numerical solutions (using the fourth-order Runge-Kutta method) was found for symmetric solutions with respect to the $Oz-$ axis. These obtained solutions can be usefully in many applications of technological interest.

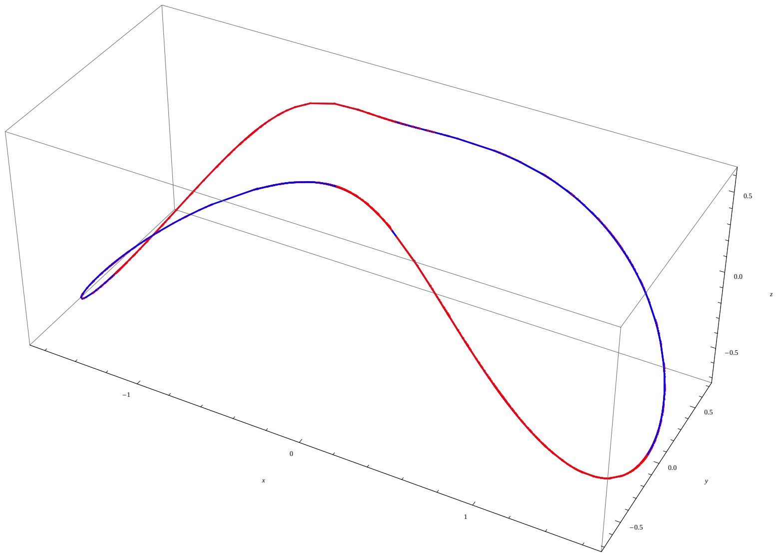

Figure 5: The parametric 3D curve $x = x(t)$, $y = y(t)$, $z = z(t)$ given by Eqs. (3), (4) using Eq. (26) with the initial conditions $x_0 = 0.5$, $y_0 = 0.5$, $z_0 = 0.5$ for $N_{max} = 25$:
OHAM solution (with lines) and numerical solution (dashing lines), respectively.

7 References

References

[1] C. Lazureanu, C. Caplescu, Stabilization of the T system by an integrable deformation, ITM Web of Conferences 34, 03009 (2020) Third ICAMNM 2020; https://doi.org/10.1051/itmconf/20203403009

[2] Braga Denis de Carvalho, Dias Fabio Scalco, Mello Luis Fernando, On the stability of the equilibria of the Rikitake system, Physics Letters A 2010; 374:4316-4320.

[3] Rikitake T., Oscillations of a system of disk dynamos, Proc. Cambridge Philos. Soc. 1958; 54:89-105.

[4] Steeb W.-H., Continuous symmetries of the Lorenz model and the Rikitake two-disc dynamo system, J. Phys. A: Math. Gen. 1982; 15:389-390.

[5] T. Binzar, C. Lazureanu, On the symmetries of a Rabinovich type system, Scient. Bull. Math.-Phys. 2012; 57(71).

[6] Lazureanu C., Binzar T., Symmetries of some classes of dynamical systems ” , Journal of Nonlinear Mathematical Physics, DOI:10.1080/14029251.2015.1033237 Corpus ID: 120157532, 2015

[7] Lazureanu C. Petrisor C., Hedrea C., On a deformed version of the two-disk dynamo system. Appl. Math. 2021; 66(3):345-372.

[8] Lazureanu C., Petrisor C., Stability and energy-Casimir Mapping for integrable deformations of the Kermack-McKendrick system. Adv. Math. Phys. 2018, Art. ID 5398768, 9 pp.

[9] Lazureanu C., Integrable deformations of three-dimensional chaotic systems. Internat. J. Bifur. Chaos Appl. Sci. Engrg. 2018; 28(5):7 pp. , Article ID 1850066, .

[10] Lazureanu C., Hamilton-Poisson realizations of the integrable deformations of the Rikitake system. Adv. Math. Phys. 2017, Art. ID 4596951, 9 pp.

[11] Lazureanu C., The real-valued Maxwell-Bloch equations with controls: from a Hamilton-Poisson system to a chaotic one. Internat. J. Bifur. Chaos Appl. Sci. Engrg. 27 (2017), no. 9, 1750143, 17 pp.

[12] Lazureanu C., On a Hamilton-Poisson approach of the Maxwell-Bloch equations with a control. Math. Phys. Anal. Geom. 20 (2017), no. 3, Paper No. 20, 22 pp.

[13] Lazureanu C., Binzar T., Symmetries and properties of the energy-Casimir mapping in the ball-plate problem. Adv. Math. Phys. 2017, Art. ID 5164602, 13 pp.

[14] Lazureanu C., Binzar T., On some properties and symmetries of the 5-dimensional Lorenz system. Math. Probl. Eng. 2015, Art. ID 438694, 7 pp.

[15] Lazureanu C., Binzar T., Symmetries of some classes of dynamical systems. J. Nonlinear Math. Phys. 22 (2015), no. 2, 265-274.

[16] Lazureanu C., Binzar T., Some symmetries of a Rossler type system. Bul. Stiint. Univ. Politeh. Timis. Ser. Mat. Fiz. 58(72) (2013), no. 2, 1-6.

[17] T. Binzar, C. Lazureanu, A Rikitake type system with one control. Discrete Contin. Dyn. Syst. Ser. B 18 (2013), no. 7, 1755-1776.

[18] Lazureanu C., Binzar T., Symplectic realizations and symmetries of a Lotka-Volterra type system. Regul. Chaotic Dyn. 18 (2013), no. 3, 203-213.

[19] T. Binzar, C. Lazureanu, On the symmetries of a Rabinovich type system. Bul. ?tiin?. Univ. Politeh. Timi?. Ser. Mat. Fiz. 57(71) (2012), no. 2, 29-36

[20] Lazureanu C., Binzar T., A Rikitake type system with quadratic control. Internat. J. Bifur. Chaos Appl. Sci. Engrg. 22 (2012), no. 11, 1250274, 14 pp.

[21] Lazureanu C., Binzar T., On the symmetries of a Rikitake type system. C. R. Math. Acad. Sci. Paris 350 (2012), no. 9-10, 529-533.

[22] Lazureanu C., On the Hamilton-Poisson realizations of the integrable deformations of the Maxwell-Bloch equations, http://dx.doi.org/10.1016/j.crma.2017.04.002, C. R. Acad. Sci. Paris, Ser. I 355 (2017) 596-600, 1631–073X/ 2017 Academie des sciences. Published by Elsevier Masson SAS.

[23] Candido Murilo R., Llibre J., Valls C., New symmetric periodic solutions for the Maxwell-Bloch differential system , Math Phys Anal Geom, 22(2), 2019, 13 pages, DOI: 10.1007/s11040-019-9313-9.

[24] David D., Holm D., Multiple Lie–Poisson structures, reduction and geometric phases for the Maxwell–Bloch traveling wave equations, J. Nonlinear Sci. 2 (1992) 241–262.

[25] Puta M., On the Maxwell–Bloch equations with one control, C. R. Acad. Sci. Paris, Serie I 318 (1994) 679–683.

[26] Puta M., Three dimensional real valued Maxwell–Bloch equations with controls, Reports on Math. Physics 3 (1996) 337–348.

[27] Arecchi F. T., Chaos and generalized multistability in quantum optics, Physica Scripta 9 (1985), 85–92.

[28] Casu I., Lazureanu C., Stability and integrability aspects for the Maxwell-Bloch equations with the rotating wave approximation, Regul. Chaotic Dyn. 22 (2017), no. 2, 109–121.

[29] Zuo D. W., Modulation instability and breathers synchronization of the nonlinear Schrodinger Maxwell–Bloch equation, Appl. Math. Lett. 79 (2018), 182–186

[30] Wang L., Wang Z. Q., Sun W. R., Shi Y. Y., Li M., Xu M., Dynamics of Peregrine combs and Peregrine walls in an inhomogeneous Hirota and Maxwell–Bloch system, Commun. Nonlinear Sci. Numer. Simul. 47 (2017), 190–199.

[31] Wei J., Wang X., Geng X., Periodic and rational solutions of the reduced Maxwell–Bloch equations, Commun. Nonlinear Sci. Numer. Simul. 59 (2018), 1–14

[32] Binzar T., Lazureanu C., On some dynamical and geometrical properties of the Maxwell–Bloch equations with a quadratic control,

https://doi.org/10.1016/j.geomphys.2013.03.016, Journal of Geometry and Physics Volume 70, August 2013, Pages 1–8

[33] Lazureanu C., The Real-Valued Maxwell–Bloch Equations with Controls: From a Hamilton-Poisson System to a Chaotic One, International Journal of Bifurcation and Chaos, 2017, Vol. 27, no 09, 773-777.

[34] Puta M., On the Maxwell-Bloch equations with one control, C.R. Acad. Sci. Paris, 1994, t. 318, Serie I, 679–683.

[35] Puta M., Integrability and geometric prequantization of the Maxwell-Bloch equations, Bull. Sci. Math, 1998, t. 122, 243–250.

[36] Puta M., Three-dimensional real-valued Maxwell-Bloch equations with controls, Reports on Mathematical Physics, 1996, Vol. 37, Issue 3, 337–348.

[37] El-Rashidy K., Seadawy Aly R., Saad Althobaiti, Makhlou M. M., Multiwave, Kinky breathers and multi-peak soliton solutions for the nonlinear Hirota dynamical system, Results in Physics 19, (2020), 7 pages, Article ID 103678, doi.org/10.1016/j.rinp.2020.103678

[38] Amer T. S., Bek M. A., Hassan S. S., Sherif Elbendary, The stability analysis for the motion of a nonlinear damped vibrating dynamical system with three-degrees-of-freedom, Results in Physics 28, (2021), 25 pages, Article ID 104561, https://doi.org/10.1016/j.rinp.2021.104561

[39] Marinca V., Herisanu N., Nonlinear dynamic analysis of an electrical machine rotor–bearing system by the optimal homotopy perturbation method, Computers and Mathematics with Applications, 61, (2011), 2019-2024.

[40] Marinca V., Ene R. D., Marinca B., Optimal Homotopy Perturbation Method for nonlinear problems with applications, Appl. Comp. Math. 2022: 21(2):123–136.

[41] Bota C., Caruntu B., Tucu D., Lapadat M., Pasca M.S., A Least Squares Differential Quadrature Method for a Class of Nonlinear Partial Differential Equations of Fractional Order, Mathematics, 8(8), 2020, Article Number 1336, DOI 10.3390/math8081336.

[42] Caruntu B., Bota C., Lapadat M., Pasca M. S., Polynomial Least Squares Method for Fractional Lane-Emden Equations, SYMMETRY–BASEL, 2019, 11(4), Article Number 479, DOI 10.3390/sym11040479.

[43] Marinca V., Draganescu G. E., Construction of approximate periodic solutions to a modified van der Pol oscillator, Nonlinear Analysis: Real World Applications, 11 (2010), 4355-4362.

[44] Herisanu N., Marinca V., Accurate analytical solutions to oscillators with discontinuities and fractional-power restoring force by means of the optimal homotopy asymptotic method, Computers and Mathematics with Applications, 60, (2010), 1607-1615.

[45] Safdar Hussain, Abdullah Shah, Sana Ayub, Asad Ullah, An approximate analytical solution of the Allen-Cahn equation using homotopy perturbation method and homotopy analysis method, Heliyon, 5, (2019), e03060.

[46] Wang X., Xu Q., Atluri S. N., Combination of the variational iteration method and numerical algorithms for nonlinear problems, Applied Mathematical Modelling, 79, (2020), 243-259.

[47] Turkyilmazoglu M., An optimal variational iteration method, Applied Mathematics Letters, 24, (2011), 762-765.

[48] Marinca V., Herisanu N. The Optimal Homotopy Asymptotic Method - Engineering Applications. Springer Verlag, Heidelberg; 2015.

Appendices

If the initial conditions are $x_0 = 0.5$, $y_0 = 0.5$ and $z_0 = 0.5$, for $N_{max} = 25$, then the approximate analytic solution $\bar{v}(t)$ given by Eq. 26 becomes:

$$\begin{aligned}
&\bar{v}(t) = \\
&= 0.7853981633 \cdot \cos(0.1212240932 \cdot t) + 1.1280863071 \cdot \cos(0.3636722796 \cdot t) - \\
&-0.3186517885 \cdot \cos(0.6061204660 \cdot t) - 0.1996129808 \cdot \cos(0.8485686525 \cdot t) - \\
&-0.2710466357 \cdot \cos(1.0910168389 \cdot t) - 0.3867642849 \cdot \cos(1.3334650253 \cdot t) - \\
&-0.1216474671 \cdot \cos(1.5759132118 \cdot t) - 0.0507600546 \cdot \cos(1.8183613982 \cdot t) + \\
&+0.0304281386 \cdot \cos(2.0608095846 \cdot t) + 0.0919966107 \cdot \cos(2.3032577711 \cdot t) + \\
&+0.0738209429 \cdot \cos(2.5457059575 \cdot t) + 0.0500084445 \cdot \cos(2.7881541439 \cdot t) + \\
&+0.0184363947 \cdot \cos(3.0306023304 \cdot t) - 0.0066048451 \cdot \cos(3.2730505168 \cdot t) - \\
&-0.0150894385 \cdot \cos(3.5154987033 \cdot t) - 0.0141512709 \cdot \cos(3.7579468897 \cdot t) - \\
&-0.0084535676 \cdot \cos(4.0003950761 \cdot t) - 0.0029454477 \cdot \cos(4.2428432626 \cdot t) + \\
&+0.0002250235 \cdot \cos(4.4852914490 \cdot t) + 0.0011645562 \cdot \cos(4.7277396354 \cdot t) + \\
&+0.0009265341 \cdot \cos(4.9701878219 \cdot t) + 0.0004806715 \cdot \cos(5.2126360083 \cdot t) + \\
&+0.0001433717 \cdot \cos(5.4550841947 \cdot t) + 0.0000179080 \cdot \cos(5.6975323812 \cdot t) - \\
&-1.648949 \cdot 10^{-6} \cdot \cos(5.9399805676 \cdot t) - 5.473392 \cdot 10^{-6} \cdot \cos(6.1824287540 \cdot t) + \\
&+4.1245926179 \cdot \sin(0.1212240932 \cdot t) + 2.7393061280 \cdot \sin(0.3636722796 \cdot t) - \\
&-1.1826779715 \cdot \sin(0.6061204660 \cdot t) - 0.4498691209 \cdot \sin(0.8485686525 \cdot t) - \\
&-0.2374141078 \cdot \sin(1.0910168389 \cdot t) - 0.1295416348 \cdot \sin(1.3334650253 \cdot t) + \\
&+0.1043902163 \cdot \sin(1.5759132118 \cdot t) + 0.1379494664 \cdot \sin(1.8183613982 \cdot t) + \\
&+0.1184346449 \cdot \sin(2.0608095846 \cdot t) + 0.0614542793 \cdot \sin(2.3032577711 \cdot t) + \\
&+0.0090494940 \cdot \sin(2.5457059575 \cdot t) - 0.0275951341 \cdot \sin(2.7881541439 \cdot t) - \\
&-0.0382993000 \cdot \sin(3.0306023304 \cdot t) - 0.0282586504 \cdot \sin(3.2730505168 \cdot t) - \\
&-0.0149834811 \cdot \sin(3.5154987033 \cdot t) - 0.0024357526 \cdot \sin(3.7579468897 \cdot t) + \\
&+0.0040036967 \cdot \sin(4.0003950761 \cdot t) + 0.0046957002 \cdot \sin(4.2428432626 \cdot t) + \\
&+0.0033601120 \cdot \sin(4.4852914490 \cdot t) + 0.0014744782 \cdot \sin(4.7277396354 \cdot t) + \\
&+0.0002834667 \cdot \sin(4.9701878219 \cdot t) - 0.0001047061 \cdot \sin(5.2126360083 \cdot t) - \\
&-0.0001492280 \cdot \sin(5.4550841947 \cdot t) - 0.0000740989 \cdot \sin(5.6975323812 \cdot t) - \\
&-0.0000204246 \cdot \sin(5.9399805676 \cdot t) - 3.372839 \cdot 10^{-6} \cdot \sin(6.1824287540 \cdot t)
\end{aligned} \tag{27}$$

 doi:10.20944/preprints202209.0474.v1

Table 1: Comparison between the first-order approximate solutions $\overline{v}$ given by Eq. 26 and numerical results for $x_0 = 0.5$, $y_0 = 0.5$ and $z_0 = 0.5$ (relative errors: $\epsilon_v = |v_{numerical} - \bar{v}_{OHAM}|$)

t	$v_{numerical}$	$\bar{v}_{OHAM}$	ϵ_v
0	0.7853981633	0.7853981633	$1.110223 \cdot 10^{-16}$
2	3.0048565944	3.0048564682	$1.262252 \cdot 10^{-7}$
4	5.4067162901	5.4067161112	$1.789394 \cdot 10^{-7}$
6	5.7469951320	5.7469952686	$1.366081 \cdot 10^{-7}$
8	4.3979496840	4.3979506058	$9.217917 \cdot 10^{-7}$
10	1.4842095296	1.4842108567	$1.327083 \cdot 10^{-6}$
12	0.4935555769	0.4935555528	$2.405788 \cdot 10^{-8}$
14	1.1089381894	1.1089371304	$1.058989 \cdot 10^{-6}$
16	3.8183645538	3.8183641247	$4.291169 \cdot 10^{-7}$
18	5.6402614592	5.6402619962	$5.369389 \cdot 10^{-7}$
20	5.6036661551	5.6036657121	$4.429515 \cdot 10^{-7}$

Table 2: Comparison between the first-order approximate solutions $\overline{v}$ given by Eq. 26 and numerical results for $x_0 = -0.5$, $y_0 = -0.5$ and $z_0 = 0.5$ (relative errors: $\epsilon_\omega = |v_{numerical} - \bar{v}_{OHAM}|$)

t	$v_{numerical}$	$\bar{v}_{OHAM}$	ϵ_v
0	-0.7853981633	-0.7853981633	$1.110223 \cdot 10^{-16}$
2	-3.0048565944	-3.0048564684	$1.260096 \cdot 10^{-7}$
4	-5.4067162901	-5.4067161110	$1.790516 \cdot 10^{-7}$
6	-5.7469951320	-5.7469952684	$1.364679 \cdot 10^{-7}$
8	-4.3979496840	-4.3979506057	$9.216750 \cdot 10^{-7}$
10	-1.4842095296	-1.4842108566	$1.326997 \cdot 10^{-6}$
12	-0.4935555769	-0.4935555528	$2.408859 \cdot 10^{-8}$
14	-1.1089381894	-1.1089371304	$1.058966 \cdot 10^{-6}$
16	-3.8183645538	-3.8183641248	$4.290359 \cdot 10^{-7}$
18	-5.6402614592	-5.6402619963	$5.370392 \cdot 10^{-7}$
20	-5.6036661551	-5.6036657119	$4.431479 \cdot 10^{-7}$

 doi:10.20944/preprints202209.0474.v1

Table 3: Values of the relative errors $\epsilon_v = |v_{numerical} - \bar{v}_{OHAM}|$ for $x_0 = 0.5$, $y_0 = 0.5$, $z_0 = 0.5$ and different values of the index number N_{max}

t	$N_{max} = 5$	$N_{max} = 10$	$N_{max} = 20$	$N_{max} = 25$
0	$1.110223 \cdot 10^{-16}$	$8.881784 \cdot 10^{-16}$	$2.220446 \cdot 10^{-16}$	$1.110223 \cdot 10^{-16}$
1/5	0.0057507451	0.0030455771	$8.383820 \cdot 10^{-4}$	$1.313631 \cdot 10^{-6}$
2/5	0.0227924915	0.0070594242	$8.097412 \cdot 10^{-4}$	$1.229725 \cdot 10^{-6}$
3/5	0.0494597939	0.0081429073	$6.156841 \cdot 10^{-5}$	$3.482073 \cdot 10^{-7}$
4/5	0.0825167222	0.0060042509	$4.729830 \cdot 10^{-4}$	$6.687728 \cdot 10^{-7}$
1	0.1176107773	0.0021559238	$1.174198 \cdot 10^{-4}$	$5.808890 \cdot 10^{-7}$
6/5	0.1499196854	0.0015691002	$4.301057 \cdot 10^{-4}$	$3.152192 \cdot 10^{-7}$
7/5	0.1749400518	0.0039327661	$6.220876 \cdot 10^{-4}$	$4.754099 \cdot 10^{-7}$
8/5	0.1892996460	0.0045783745	$4.222215 \cdot 10^{-4}$	$1.913513 \cdot 10^{-7}$
9/5	0.1914052506	0.0038272807	$1.319308 \cdot 10^{-4}$	$2.917863 \cdot 10^{-7}$
2	0.1817135046	0.0022665042	$5.933946 \cdot 10^{-6}$	$1.262252 \cdot 10^{-7}$